On Instability of Acoustic Waves Propagating in Stratified Vortical Flows*

Igor MEN'SHOV** and Yoshiaki NAKAMURA***

The propagation of sound waves in a finite vortex is investigated by numerically solving the linearized Euler equations in two dimensions. Two types of vortices are considered: homentropic, when the entropy is uniformly distributed in space, and non-homentropic, or entropy stratified, when it is distributed non-uniformly. In the latter case, the results reveal instability of the perturbation field, which is caused by entropy-rotational waves excited in the vortex region by incident sound waves.

Key Words: stratified vortex, scattering, sound waves, linearized Euler equations.

1. Introduction

The problem to be studied in the present paper is the scattering of sound waves by a vortex. This problem has received significant attention recently in relation to the prediction of sound produced by turbulent flows. This problem can also be considered as a simple model for sound wave scattering by turbulent shear flows with large-scale vortical structures that are dominant in the wake flow. Therefore, vortex scattering is also associated with the detection of trailing vortices behind flying bodies. Finally, as can be seen from the present research, this problem has particular concern with hydrodynamic instability of vortical flows.

In most papers published until the present [1-3] the scattering problem is considered under the assumption that the base flow in the vortex is homentropic; i.e. it is characterized by a constant distribution of entropy in space. In this case no entropy-rotational perturbation field can be generated. The field of perturbations is always adiabatic and irrotational so that the perturbation pressure $\hat{p}$ is related to the perturbation density $\hat{\rho}$ by $\hat{p} = c^2\hat{\rho}$, where c is the sound velocity in the base flow, and the perturbation velocity $\hat{\mathbf{V}}$ is defined by a potential function $\hat{\varphi}$ as $\hat{\mathbf{V}} = grad(\hat{\varphi})$.

If the base flow is not homentropic, i. e. there is stratification in the entropy distribution, the propagation of sound waves is accompanied by the generation of entropy-rotational waves in the perturbation field, which can essentially affect the process of sound propagation. In the present study we make an attempt to investigate this phenomenon numerically by considering the scattering of adiabatic sound waves by an entropy stratified vortex.

* Received on July 31, 2001.

** Lecturer, e-mail: menshov@nuae.nagoya-u.ac.jp
*** Professor, e-mail: nakamura@nuae.nagoya-u.ac.jp
Depart. of Aerospace Engineering., Nagoya University, Furo-cho, Chikusa-ku, Nagoya 464-8603, Japan.

2. Problem Statement

We consider the propagation of sound waves in a base flow that is assumed to be steady and not affected by the perturbation field. This base flow is represented by a circular isolated vortex, where the distribution of state parameters in the radial direction is taken so as to follow the two-dimensional Euler equations.

Two vortical flows are considered here. One is a homentropic vortex, when the pressure and density are related such that the gas entropy has a constant distribution in space. The other is an entropy-stratified vortex with a nonconstant distribution of entropy. For the both cases, the velocity field of the base flow is taken in such a way that it decays exponentially fast as we go away from the vortex center. Such azimuthal velocity distribution has been used in several recent papers, for example [1]. Specifically, the distributions we use in the present calculations are as follows:

$$u_r = 0,\ \ u_\varphi = 2\frac{r}{a}\mu z,\ \ z = \exp\left[-\left(\frac{r}{a}\right)^2\right] \qquad (1)$$

$$p = p_\infty \left\{ 1 - \frac{\gamma - 1}{\gamma} \frac{\rho_\infty}{p_\infty} \mu^2 \left[1 + \frac{2\theta}{2+\alpha} z^\alpha \right] z^2 \right\}^{\frac{\gamma}{\gamma-1}}$$

$$s = 1 + \theta z^\alpha,\ \rho = \rho_\infty \cdot s \cdot \left(\frac{p}{p_\infty} \right)^{1/\gamma}$$

Here a is the reference radius of the vortex, μ is the vortex intensity that is proportional to the maximal azimuthal velocity, γ is the constant ratio of specific heats. The parameters θ and α in eq. (1) specify the entropy distribution. If $\theta=0$, it corresponds to the case of a homentropic vortex.

A schematic drawing of the flow configuration is shown in Fig. 1. The calculation domain is a square with a non-dimensional length $L=5$, with the vortex core radius a being taken as the reference length. Sound waves are irradiated by a speaker or vibrator, a short rigid plate, that executes small harmonic oscillations with a prescribed velocity $u_w = U_0 \cos(\omega \cdot t)$ in the direction normal to the left boundary of the computational domain, as shown in Fig. 1. The length of the vibrator is *5%* of L, and it is located at the middle of the left boundary.

All boundaries of the computational domain except for the location of the speaker are treated as non-reflecting by implementing characteristic boundary conditions. A uniform grid is used in calculations, which consists of *201* evenly spaced cells in each direction.

3. Calculation Method

To calculate the scattering problem stated above we employ a method that is based on the Linearized Euler Equations (LEE). The LEE model is commonly used for aeroacoustic problems [4,5]. However, the present approach differs from those common methods. The main distinctive feature of this approach is that the linearization is carried out for the discretized equations rather than the differential ones. Futhermore, the numerical perturbation flux is approximated by using the exact solution to the Variational Riemann problem (VRP) [6], which is an application of the RP to the equations of small perturbation dynamics.

We start with the compressible Navier-Stokes equations discretized in space with the finite volume method on a given computational grid,

$$\omega_i \frac{d\mathbf{q}_i}{dt} + \sum_\sigma s_\sigma T_\sigma^{-1} \mathbf{f}_\sigma(\mathbf{q}) = \sum_\sigma s_\sigma \mathbf{g}_\sigma(\mathbf{q}) \qquad (2)$$

where $\mathbf{q}_i$ is the cell average value of the vector of conservative variables, ω_i is the cell volume, s_σ is the area of the cell interface, $\mathbf{f}_\sigma(\mathbf{q})$ is the local one-dimensional inviscid flux averaged over the interface, T_σ is the transforming matrix defined by unit vectors of the interface local basis, $\mathbf{g}_\sigma(\mathbf{q})$ is the interface averaged viscous flux. The summation in eq. (2) is performed over all interfaces surrounding the cell under consideration.

Then the flow parameters are decomposed into a mean, or base flow component, and a perturbation component,

$$\mathbf{q} = \bar{\mathbf{q}} + \hat{\mathbf{q}} \qquad (3)$$

where the mean flow parameters are supposed to satisfy the semi-discrete equation (2). Due to the decomposition (3), the fluxes in eq. (2) can be written as

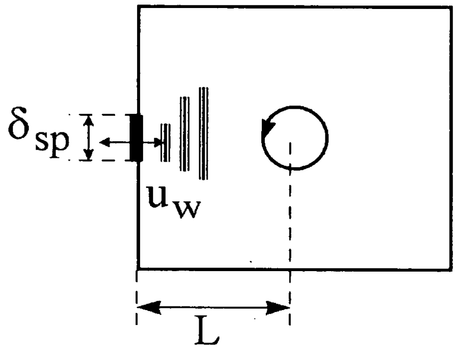

Fig. 1. Schematic configuration for sound scattering computations

the summation of three contributions: the mean flow flux, (̄), the perturbation flux including only linear terms with respect to components of the perturbation vector, (̂), and the non-linear perturbation flux, (̃), i.e.

$$\mathbf{f}_\sigma = \bar{\mathbf{f}}_\sigma + \hat{\mathbf{f}}_\sigma + \tilde{\mathbf{f}}_\sigma,\quad \mathbf{g}_\sigma = \bar{\mathbf{g}}_\sigma + \hat{\mathbf{g}}_\sigma + \tilde{\mathbf{g}}_\sigma \qquad (4)$$

The LEE model for the propagation of perturbations is obtained under the assumption [4, 5] that the viscous perturbation fluxes $\hat{\mathbf{g}}_\sigma, \tilde{\mathbf{g}}_\sigma$ can be neglected, and non-linear inviscid perturbation terms, which are mostly responsible for sound generation processes, are modeled by a volume source term $\mathbf{S}$ for the disturbance production. This term is commonly derived by using some semi-empirical models constructed on the base of available experimental data. With the above assumptions, the discrete model for the evolution of a perturbation field against the background of a given mean flow takes the following form:

$$\omega_i \frac{d\hat{\mathbf{q}}_i}{dt} + \sum_\sigma s_\sigma T_\sigma^{-1} \hat{\mathbf{f}}_\sigma(\bar{\mathbf{q}}, \hat{\mathbf{q}}) = \omega_i \mathbf{S}_i \qquad (5)$$

The key point of the present approach is the approximation of the perturbation flux $\hat{\mathbf{f}}_\sigma$. We treat this flux in view of the Godunov method as the resultant flux at the cell interface arising from the interaction of perturbations in two neighbouring cells. Let $\sigma(i)$ be the order number of the cell bordering the current cell i on the interface σ. Then the acoustic flux can be written in terms of the solution to the VRP as

$$\hat{\mathbf{f}}_\sigma = A(\overline{\mathbf{Q}}^R_\sigma)\hat{\mathbf{Q}}^R_\sigma \tag{6}$$

where A is the Jacobian of the inviscid flux evaluated at the exact solution to the RP, $\overline{\mathbf{Q}}^R_\sigma$, and $\hat{\mathbf{Q}}^R_\sigma$ is the variation of this solution caused by the cell perturbations. Here the vector **Q** is related to the vector **q** by the interface-based transforming matrix T as **Q**=T**q**.

The solution to the VRP, $\hat{\mathbf{Q}}^R_\sigma$, is expressed through variational matrices M_i and $M_{\sigma(i)}$, which have been obtained in [6], as follows:

$$\hat{\mathbf{Q}}^R_\sigma = M_i\hat{\mathbf{Q}}^\sigma_i + M_{\sigma(i)}\hat{\mathbf{Q}}^\sigma_{\sigma(i)} \tag{7}$$

Here the superscript σ implies that the vectors of perturbations are evaluated at the center of the interface. The first order scheme is obtained, if a constant function is used for the distribution of perturbations within the cell, $\hat{\mathbf{Q}}^\sigma_i = \hat{\mathbf{Q}}_i$. To enhance the accuracy of the method, the disturbance vector of primitive variables is assumed to be a linear function in space within each computational cell [7], and a MUSCL-type approach [8] is applied to calculate the interface values.

With the use of eqs. (6) and (7), the eq. (5) can be written in the following convenient form:

$$\frac{d\hat{\mathbf{q}}_i}{dt} = \mathbf{R}_i(\hat{\mathbf{q}})$$
$$\mathbf{R}_i(\mathbf{q}) = \mathbf{S}_i - \tag{8}$$
$$-\frac{1}{\omega_i}\sum_\sigma s_\sigma T^{-1}_\sigma A(\overline{\mathbf{Q}}^R_\sigma)\left[M_i T_\sigma \hat{\mathbf{q}}^\sigma_i + M_{\sigma(i)} T_\sigma \hat{\mathbf{q}}^\sigma_{\sigma(i)}\right]$$

For the time discretization of these equations, a low storage 3^{rd} order Runge-Kutta scheme is applied as follows:

$$\hat{\mathbf{q}}^{(1)}_i = \hat{\mathbf{q}}^n_i + \frac{1}{3}\Delta t\mathbf{R}_i(\hat{\mathbf{q}}^n)$$
$$\hat{\mathbf{q}}^{(2)}_i = \hat{\mathbf{q}}^n_i + \frac{2}{3}\Delta t\mathbf{R}_i(\hat{\mathbf{q}}^{(1)}) \tag{9}$$
$$\hat{\mathbf{q}}^{n+1}_i = \hat{\mathbf{q}}^n_i + \frac{1}{4}\Delta t\mathbf{R}_i(\hat{\mathbf{q}}^n) + \frac{3}{4}\Delta t\mathbf{R}_i(\hat{\mathbf{q}}^{(2)})$$

where Δt is the time step.

4. Numerical Results

The linear stability theory of inviscid swirling flows has mainly been developed in the last three decades. Many stability conditions have been obtained for rotating liquids and gases in confined domains (see for example, [9] and references therein). However, little is known about stability of unconfined compressible vortices, in particular vortices with a stratification of entropy. Thus, the linear stability analysis presented in [10] shows only neutrally stable modes for the compressible homentropic vortex with a Gaussian vorticity profile, which is also studied in the present paper. The effect of entropy stratification is also investigated in [10] for a particular entropy profile. The results obtained indicate that a positive entropy gradient can destabilize the vortex, while a negative one has the opposite effect.

We study this stability problem by investigating the perturbation field that arises when sound waves run into a vortex. Calculations have been carried out under different conditions that are characterized by two parameters. One is the non-dimensional intensity of the base vortex $\overline{\mu}$, which is defined as $\overline{\mu} = \mu\sqrt{\rho_\infty / p_\infty}$. The other is parameter δ that equals the ratio between the wavelength of incident waves λ and the vortex radius a, i.e., $\delta=\lambda/a$. It is assumed that there is no any perturbation field in the computational domain at the initial time moment, i.e., $\hat{\mathbf{q}} = 0$ at $t=0$. The acoustic source term S at the right-hand side of eq. (5) is neglected in the present study.

4.1 Scattering by homentropic vortex

First, we present numerical results of the sound scattering by a homentropic vortex when the parameter θ in eqs. (1) vanishes. In Fig. 2 computed acoustic pressure contours and velocity vectors are shown for the case $\overline{\mu}=0.5$ that corresponds to the maximal Mach number in the vortex of *0.1365*. The frequency of incident sound waves is $\omega=4\pi$, which corresponds to the case $\delta=0.64$. The state shown in this figure responds to a rather large time moment $t=562$, when the speaker has executed more than *1000* oscillations.

These results definitely exhibit a typical pattern of the scattering of sound waves by an isentropic finite vortex [1, 3]. The scattered field is monochromatic with the same frequency as the incident waves in this case. Therefore, the total, i.e., incident plus scattered, field has to be also monochromatic of the same frequency. This is clearly illustrated in Fig. 3, where the time history of the perturbation pressure is shown for a reference point located behind the vortex at a distance $r=1$ from the vortex center.

4.2 Instabilities of the perturbation field when scattering by stratified vortex

The numerical results shown below have been obtained for the scattering of sound waves by a stratified vortex with the following flow conditions: $\alpha=1.5$, $\theta=-0.5$, $\overline{\mu}=0.5$ (maximal Mach number equals 0.105, a positive entropy gradient). Incident sound waves were generated by a low frequency speaker of $\omega=0.05\pi$ ($\delta=51.2$).

In Fig. 4 the perturbation pressure is shown for this case at 3 non-dimensional time moments: $t_1 = 28.7, t_2 = 57.4$, and $t_3 = 86.1$, which correspond to $0.7T$, $1.4T$, and $2.1T$, respectively. Here T is the period of speaker oscillations, and the elapsed time is measured from the moment when the speaker starts generating sound waves.

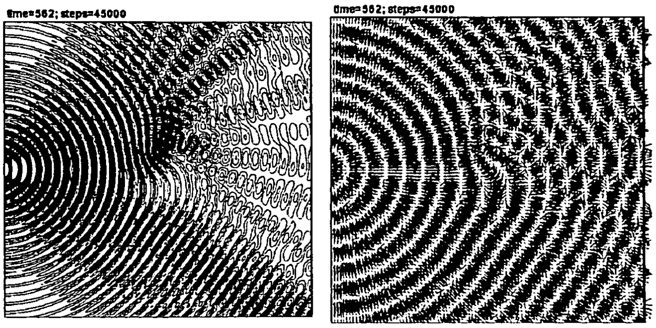

Fig. 2. The scattering of sound waves by a homentropic vortex; acoustic pressure contours with p_{min}=-5e-4 and p_{max}=5e-4 (left) and velocity vectors (right).

Unlike the homentropic vortex case, the scattering of the acoustic field by the stratified vortex is accompanied by the formation of two entropy-rotational waves in the perturbation field in the core of the vortex, as seen in Fig. 4. One wave has a relatively high pressure, and the other has a low pressure. We refer to these waves as plus-minus waves, respectively.

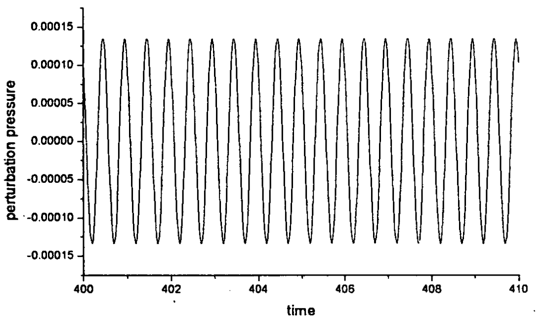

Fig. 3. Pressure time history at a reference point (-1,0) for homentropic vortex.

By the time moment $t \approx 70$ this couple of plus-minus waves breaks into two couples of symmetrical plus-minus waves centered approximately at the distance $r=1$ from the vortex center. The perturbation velocity field becomes distinctly rotational, which is represented by four vortices, as seen in Fig. 5.

At later times this four-leafed structure of waves reveals all attributes of hydrodynamic instability. This is characterised by intensive amplification of the amplitude of all parameters, which can be seen, for example, in the distribution of the perturbation pressure versus non-dimensional time presented in Fig. 6 for three reference points. These points are taken behind the vortex at distances $r=1,\ 3,\ 4$ from the vortex center, respectively. The total perturbation energy, which is defined by second order terms of a power series in the perturbation parameters of the gas total energy, in the vortex region, $|r|<1$, versus time is given in Fig. 7 on a logarithmic scale, which clearly exhibits a linear dependence between these two parameters. This shows a typical feature of hydrodynamic instability when the perturbation energy exponentially increases with time. Note that the existence of similar rotating waves has been also found in [10] for a homentropic Gaussian vortex. However, these waves appeared to be neutrally stable.

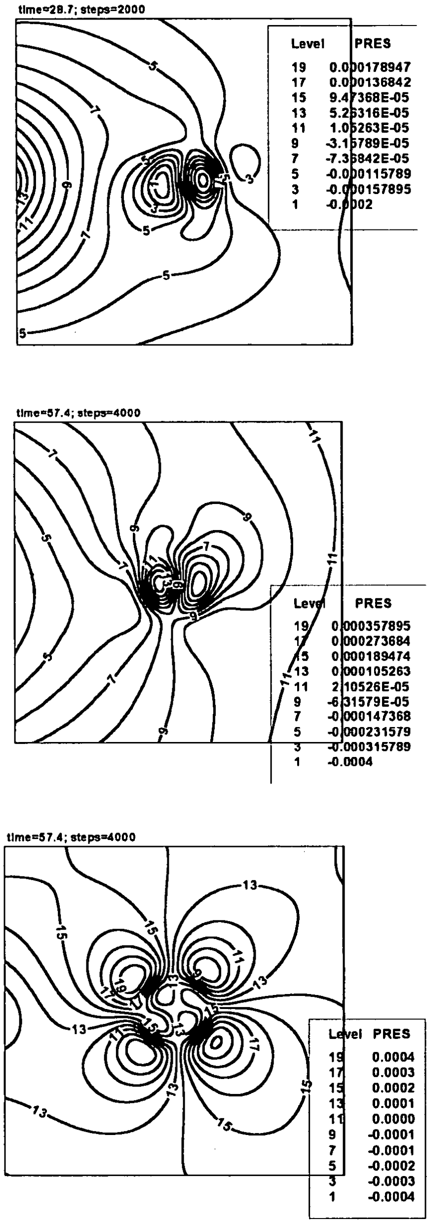

Fig. 4. Pressure perturbation contours at 3 time moments for scattering by entropy-stratified vortex.

The perturbation velocity vector presented in Fig. 5 clearly reveals that this instability is accompanied by the formation of a regular structure, which consists of four focus-type points located along the vortex periphery and one saddle-type point in the vortex center for the flow conditions under consideration.

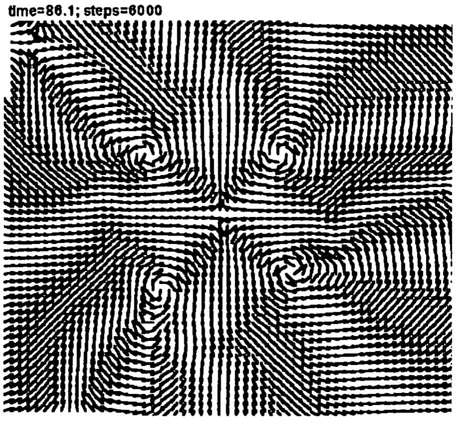

Fig. 5. Acoustic velocity vectors for the scattering by non-homentropic vortex.

The same type of instability is found for different vortex intensities. Figures 8a, 8b, and 8c display time histories of the perturbation pressure at the reference points, $r=1, 3, 4$, for sound waves with the frequency $\omega = 0.1\pi$ and the vortex intensity $\overline{\mu} = 0.5, 1, and\ 1.2$, respectively. The total perturbation energy in the vortex region $|r|<1$ for these three cases is shown in Fig. 9.

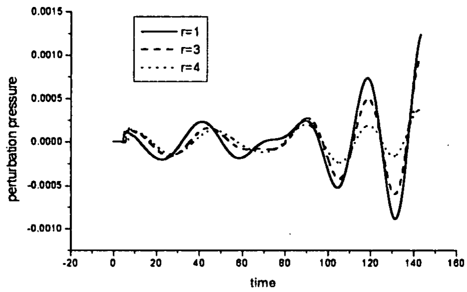

Fig. 6. Time history of pressure for different reference points located behind vortex.

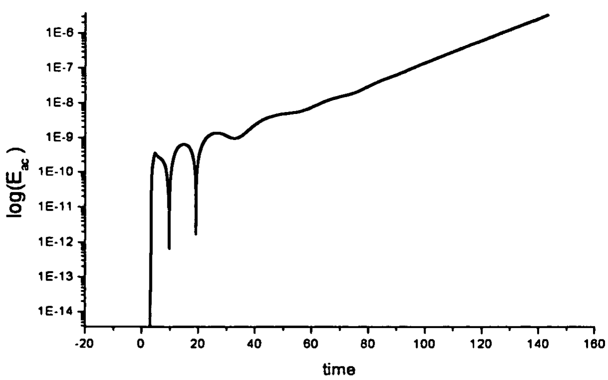

Fig. 7. Perturbation energy for $|r|<1$ versus time.

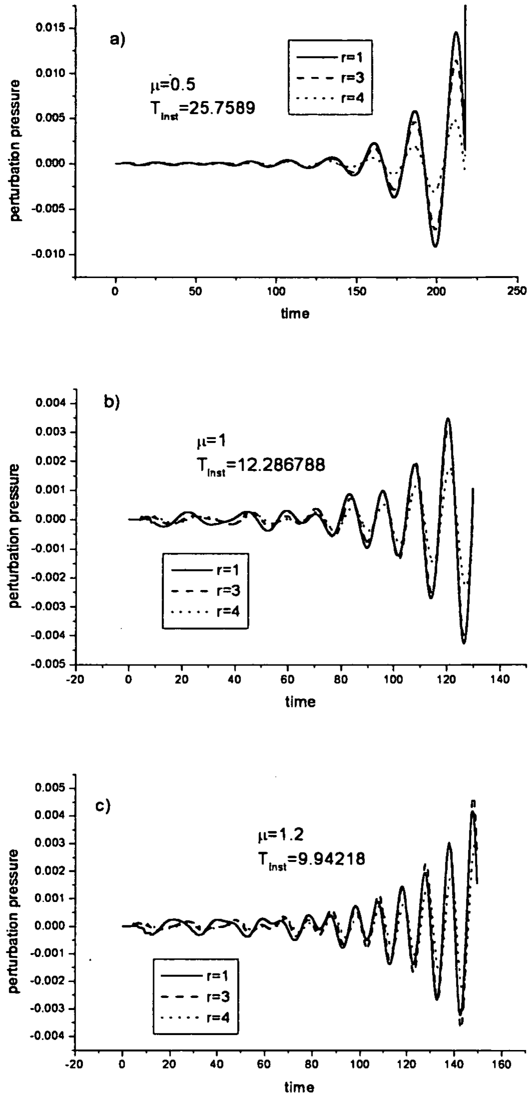

Fig. 8. Time history of the perturbation pressure.

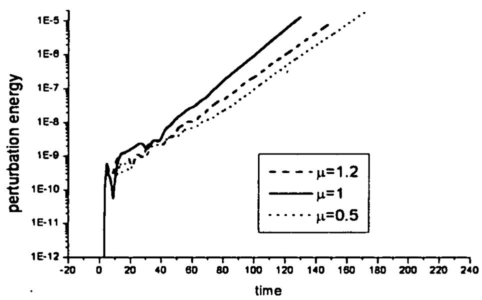

Fig. 9. Perturbation energy for $|r|<1$ versus time.

The instability evolution depends on the frequency of incident sound waves. This is illustrated in Fig. 10, where the total perturbation energy is displayed versus non-dimensional time for the vortex intensity $\overline{\mu} = 1$ and a frequency of incident sound waves of 0.1π, 0.3π, 2π, and 4π, respectively. As can be seen from this figure, the longer incident waves become, as the shorter irradiation time is required for the instability excitation.

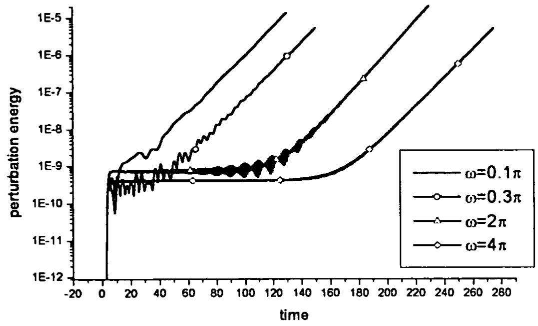

Fig. 10. Perturbation energy of the vortex region versus time under different incident wave conditions.

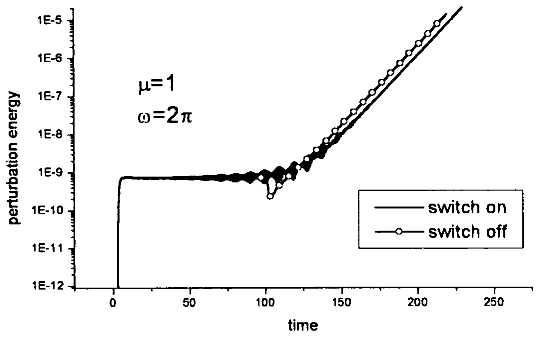

Fig. 11. Self-exciting instability.

Once it appears, the instability structure becomes self-exciting, and does not vanish, even if the vibrator is switched off. Figure 11 shows calculated results for the case $\bar{\mu} = 1$ and $\omega = 2\pi$, where the speaker is intentionally turned off at the beginning of the instability excitation (t=94.7). It is seen that the evolution of the perturbation field in the vortex region in the case of switched-off speaker almost exactly follows that in the case of switched-on speaker. This means that there is no longer influence of incident sound waves on the perturbation field in the vortex, and the evolution of entropy-rotational waves is a self-exciting, vortex intrinsic unstable process.

5. Conclusion

The scattering of sound waves by a homentropic and an entropy-stratified finite vortex has been numerically investigated by solving the LEE. Analysis of these calculations allows us to infer the following conclusions.

a) The scattering of sound waves by the homentropic vortex does not induce any instabilities, and the computed scattered acoustic field exhibits the same characteristics as predicted by both analytical and another numerical methods.

b)The perturbation field in the case of stratified vortex becomes unstable; that is, an unlimited increase in the amplitude of all parameters (such as perturbation pressure, velocity, and density) is observed. This instability is caused by entropy-rotational perturbation waves excited in the vortex core by incident adiabatic sound waves.

c) This instability is accompanied by the formation of a regular structure in the spatial distribution of perturbation parameters in the vortex region, where the distribution is distinctly periodical in the angular variable.

d) Once it appears, the instability becomes self-exciting, and doesn't depend on incident sound waves.

References

(1) Colonius, T., Lele, K. and Moin, P, "The scattering of sound waves by a vortex: numerical simulations and analytical solutions", J.Fluid.Mech., **260** (1994), pp. 271-298.

(2) Ford, R., Llewellyn Smith, S. G., "Scattering of acoustic waves by a vortex", J. Fluid Mech., **386** (1999), pp. 305-328.

(3) Berthet, R., Astruc, D., and Estivalezes, J. L., "Assessment of numerical boundary conditions for simulation of sound scattering by vorticity", AIAA Paper 2000-2005, 2000.

(4) Mankbadi, R.R., Hixon, R., Shin, S.-H., Povinelly, L.A., "Use of Linearized Euler Equations for Supersonic Jet Noise Prediction", AIAA J., **36** (1998), No. 2, pp. 140-146.

(5) Bailly, C., Bogey C., and Juve, D., "Computation of flow noise using source terms in linearized Euler equations", AIAA Paper 2000-2047, 2000.

(6) Men'shov, I. and Nakamura, Y., "On implicit Godunov's method with exactly linearized numerical flux", Computers & Fluids, **29**(2000), pp.595-616.

(7) Barth, T.J., Frederickson, P.O., "Higher Order Solution of the Euler Equations on Unstructured Grids Using Quadratic Reconstruction", AIAA Paper, 90-0013, (1990).

(8) B. van Leer, "Toward the ultimate conservative difference scheme", II, J.Comput.Phys., **14** (1979), pp. 361-382.

(9) Hultgren, L, "Stability of swirling gas flows", Phys.Fluids, **31**, 7, (1988), pp.1872-1876.

(10) Chan, W.M., Shariff, K., and Pulliam, T.H., "Instabilities of two-dimensional inviscid compressible vortices", J. Fluid Mech.,**253**, (1993), pp.173-209.